ISSN 1027-5495. Functional Materials, 24, No.1 (2017), p. 52-55.
doi:https://doi.org/10.15407/fm24.01.052

Influence of gas adsorption on the impedance of porous GaAs

***Y.S.Milovanov*[1], *I.V.Gavrilchenko*[1], *S.V.Kondratenko*[1], *A.P.Oksanich*[2], *S.E.Pritchin*[2], *M.G.Kogdas*[2]**

[1]Institute of High Technologies, T.Shevchenko National University of Kyiv, 64 Volodymyrska Str., 06001 Kyiv, Ukraine
[2]Kremenchuk M.Ostrohradskyi National University, 20 Pershotravneva Str. 39600 Kremenchuk, Ukraine

Received November 7, 2016

Porous GaAs was formed electrochemically on *n*-type GaAs in a HF:C_2H_5OH (1:3) electrolyte. The surface morphology of porous GaAs has been studied using atomic force microscopy (AFM). The hodographs of the total impedance and the adsorption influence of ethanol and acetone vapor on the charge transfer were examined.
Keywords: Porous GaAs, AFM, impedance spectroscopy, Nyquist plots.

Пористый GaAs сформирован электрохимически на GaAs *n*-типа в электролите HF:C_2H_5OH (1:3). Морфология поверхности пористого GaAs изучена с помощью атомно-силовой микроскопии. Исследованы годографы полного импеданса и адсорбционное влияние паров этанола и ацетона на перенос заряда.

Вплив адсорбції газу на импеданс поруватого GaAs. *Ю.С.Мілованов, І.В.Гаврильченко, С.В.Кондратенко, А.П.Оксаніч, С.Е.Прітчін, М.Г.Когдас.*
Пористий GaAs сформований електрохімічно на GaAs *n*-типу в електроліті HF:C_2H_5OH (1:3). Морфологію поверхні пористого GaAs вивчено за допомогою атомно-силової мікроскопії. Досліджено годографи повного імпедансу та адсорбційний вплив парів етанолу та ацетону на перенос заряду.

1. Introduction

Although porous silicon has attracted preferential attention into optoelectronic applications since the discovery of the phenomenon of photoluminescence at room temperature in 1990 [1], there has been also increasing interest in employing porous silicon and its large internal surface area in the field of sensor technology. Porous silicon was shown to be very sensitive to the gas ambient. A set of electrical [2–5], luminescent [6–8] and optical [9, 10] transducer principles have been already used for gas detection. The effects observed could be measured by several decimal orders. However, not solved yet problem of porous silicon application remains the instable optical and electrical characteristics due to ageing, illumination, exposition to ambient gases etc. [11, 12]. That why to develop the improved sensors of high sensitivity and selectivity it is necessary to search new nano materials.

Well known that anodisation results in formation of porous GaAs layers with luminescence in the visible region, at higher energies than porous silicon [13–15].

It was found that porous GaAs shows good sensing properties toward H_2 [16]. But for the moment the porous GaAs is not well investigated for sensor application that's why it is necessary to study the influence of different gas adsorption on the its electrical

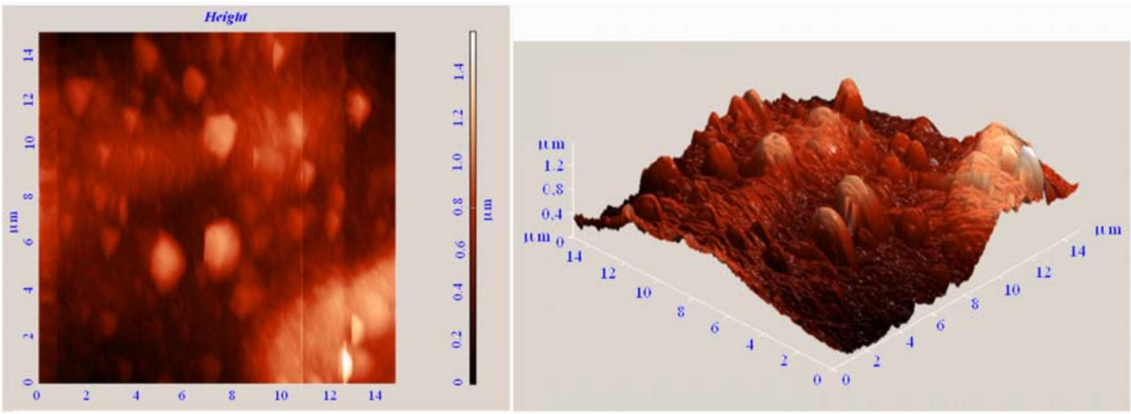

Fig. 1. AFM image of the n-type porous GaAs layer (a) 2D view (b) 3D view.

properties. In the present work we analyzed the adsorption influence of ethanol and acetone vapor on the electrical properties of porous GaAs by the method of impedance spectroscopy.

2. Experimental

Porous GaAs is produced by electrochemical etching of (100) n-type GaAs, doped with Sn. The etching is carried out in HF and ethanol mixture under galvanostatic condition. The sample is etched in a $HF:C_2H_5OH = 1:3$ solution at current density 25 $mA \cdot cm^{-2}$ for 5 min. The anodisation is produced in a Teflon electrochemical cell. Firstly, before processing, the n-GaAs is conventionally cleaned with acetone and deionised water. In order to investigate the electrical properties metal contact dots are formed by evaporating silver (Ag), as circle dots with a diameter of about 1 mm on the front surfaces of n-type porous GaAs, by using a vacuum evaporation technique.

Atomic force microscopy is used to examine surface morphology. Impedance spectroscopy [17, 18] was used to study the sample's electrical properties. The impedance spectra were measured at room temperature using Z-2000 impedance meter at *ac* current mode in the frequency range from 10 to $2 \cdot 10^6$ Hz. During measurements the *ac* voltage amplitude was 100 mV, the error didn't exceed 5 %. The detail of analysis of impedance curves of dispersed semiconductors applied in this work can be found in [19, 20]. Ethanol and acetone were investigated in saturated vapor form by pumping through the bubbler.

3. Results and discussion

The surface morphology of porous substrate has been studied using atomic-force

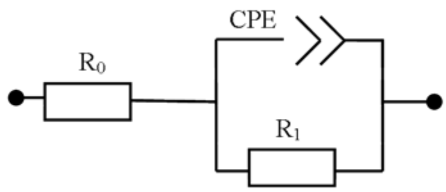

Fig. 2. Equivalent schema.

microscopy using a scanning area of 14×14 μm^2. Fig. 1 shows the AFM imaging (a) 2D view and (b) 3D view of the porous GaAs surface. The porous GaAs layer exhibits a not homogenous nanostructured surface morphology, which consists of pyramid shaped crystallites and micro- and nanopores.

The impedance spectra of n-type porous GaAs samples in dry air is presented in Fig. 3. As can be seen, the Nyquist plot (total impedance of the device) consists of one non ideal semicircle in frequency range of 10–2 MHz.

The experimental data of impedance spectroscopy are interpreted in terms of an equivalent electrical circuit based on a probable physical model, each element of which characterizes electrochemical properties of the porous layers, their structural peculiarities, or physical-chemical processes occurring in the system under study.

In order to describe the resistive-capacitive properties of the porous materials in the equivalent electrical circuit, a constant phase element (CPE) is used (Fig. 2). Introducing the CPE is a standard operation when modeling the impedance for a wide class of systems with exponential distribution of the parameters associated with overcoming the energy barrier in the process of charge transfer; the CPE describes the behavior of the impedance, which is induced

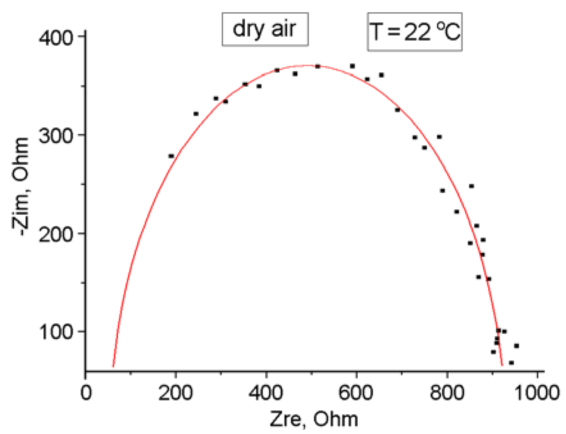

Fig. 3. Nyquist plots of n-type porous GaAs in dry air. Points are experiments, lines are calculation.

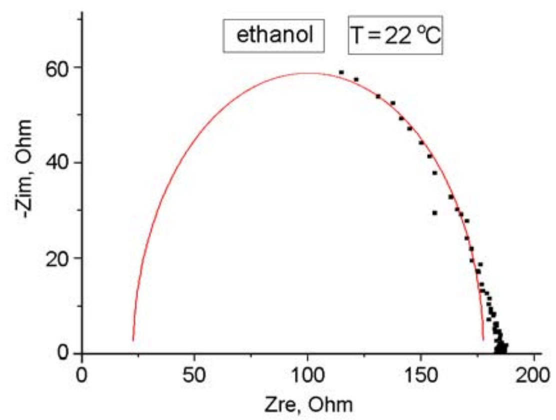

Fig. 4. Nyquist plots of n-type porous GaAs in saturated vapor of ethanol. Points are experiments, lines are calculation.

by the manifestation of the fractal properties of the structures under study in a certain frequency range. An impedance element Z in this case takes the form of:

$$Z = \frac{1}{A(j\omega)^n}, \quad (1)$$

where A is a proportionality coefficient, n is the exponential index responsible for phase shift ($-1 \le n \le 1$), and j is the imaginary unit.

The pre-exponential coefficient A has a capacitive dimension. For total values n = 1, 0, −1 element CPE is degenerated to classical elements with the following parameters: capacity C, resistance R, and inductivity L, respectively. While $n = 0.5$, part with constant phase is Warburg element W.Change of the value of exponential coefficient independent of frequency, can be associated with a total effect of reducing the volume of charge space area at the grain boundaries, flow channel modelling, repolarization of the surface states, etc. The principle of work of semiconductors gas sensors with porous GaAs layer is based on the change of their electrical conductivity during gas adsorption. These changes are primarily due to changes in the concentrations of electrons in the conductive band (or holes in valence band) as a result of the

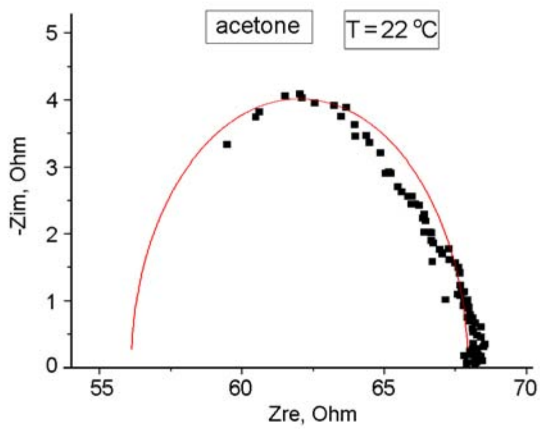

Fig. 5. Nyquist plots of n-type porous GaAs in saturated vapor of acetone. Points are experiments, lines are calculation.

exchange of charge with adsorbed particles of gas phase.

The impedance hodographs constructed for the circuit consist of resistor R and the CPE, which are connected in parallel. The parameters of approximations for this model (Fig. 2) are presented in Table. For this circuit, the characteristic charge accumulation time can be written as:

$$\tau = (RA)^{1/n} = \frac{1}{\omega} = \frac{1}{2\pi f_{max}}, \quad (2)$$

Table. Parameters of approximations

Atmosphere	Parameters				
	R_0 (Ω)	R_1 (Ω)	n	F_{max} (kHz)	τ (μs)
Dry air	55	870	0,85	80	2
Saturated vapor of ethanol	22	155	0.76	2000	0,08
Saturated vapor of acetone	56	11	0.68	1200	0.13

where ω is the angular frequency for the maximum reactive component of the complex impedance (at the point of maximum relaxation on the impedance hodograph).

Figure 4 and 5 shows the Nyquist curves of a sample in a saturated vapor of ethanol and acetone. As can be seen, the adsorption of saturated vapor of ethanol and acetone results in the shifting of Nyquist curves along the real axis toward lower values of Z_{Re}. It is found that in the presence of gases the resistance R_1 is decreased, i.e., the height of a segment and the circle radius decrease and the relaxation maximum shifts to the region of higher frequencies (see Table). This is due to the combined effect of reducing the depleted charge region and the modulation of the flow and recharge channels of the surface states.

4. Conclusions

Porous GaAs was formed electrochemically on n-type GaAs in a $HF:C_2H_5OH$ (1:3) electrolyte. The impedance spectroscopy was applied for analysis of porous layer. It was found that the impedance spectroscopy results can be interpreted using a single R-CPE equivalent circuit model.

The adsorption influence of ethanol and acetone vapor on the electrical properties of porous GaAs was studied. It is also found that, in the presence of gases the relaxation maximum in the Nyquist plots shifts to the region of higher frequencies.

References

1. L.T.Canham, *Appl. Phys. Lett.*, **57**, 1046 (1990).
2. V.G.Litovchenko, T.I.Gorbanyuk, V.S.Solntsev et al., *Appl. Surf. Sci.*, **234**, 262 (2004).
3. V.Strikha, V.Skryshevsky, V.Polishchuk et al., *J. Porous Mat.*, **7**, 111 (2000).
4. Z.Gaburro, P.Bettotti, Saiani et al., *Appl. Phys. Lett.*, **85**, 555 (2004).
5. V.A.Vikulov, V.I.Strikha, V.A.Skryshevsky et al., *J. Phys. D*, **33**, 1957 (2001).
6. T.Dittrich, E.A.Konstantinova, V.Ya.Timoshenko, *Thin Solid Films*, **255**, 238 (1995).
7. T.Serdiuk, V.A.Skryshevsky, I.I.Ivanov et al., *Mater. Lett.*, **65**, 2514 (2011).
8. S.Fellah, F.Ozanam, N.Gabouze et al., *Phys. Stat. Sol. A*, **182**, 367 (2000).
9. I.I.Ivanov, V.A.Skryshevsky, T.Serdiuk et al., *Sensors and Actuators B*, **174**, 521 (2012).
10. S.Chan, P.M.Fauchet, Y.Li et al., *Phys. Stat. Solidi. A*, **182**, 541 (2000).
11. A.Benilov, I.Gavrilchenko, I.Benilova et al., *Sensors and Actuators A*, **137**, 345 (2007).
12. V.Lysenko, V.Onyskevych, O.Marty et al., *Appl. Phys. Let.*, **92**, 251910 (2008).
13. P.Schmuki, D.J.Lockwood, H.J.Labbe et al., *Appl. Phys. Lett.*, **69**, 1620 (1996).
14. M.Naddaf, S.Saloum, *Physica E*, **41**, 1784 (2009).
15. H.Saghrouni, A.Missaoui, R.Hannachi et al., *Superlattices and Microstructures*, **64**, 507 (2013).
16. A.Salehi, A.Nikfarjam, D.J.Kalantari, *Sensors and Actuators B*, **113**, 419 (2006).
17. JR Mac Donald, Impedance Spectroscopy e Emphasizing Solid Materials and Systems, Wiley, New York (1987).
18. E.E.Barsoukov, J.R.Macdonald, Impedance Spectroscopy: Theory, Experiment, and Applications, Wiley, New York (2005).
19. Y.S.Milovanov, I.V.Gavrilchenko, V.Y.Gayvoronsky et al., *J. Nanoelectron. Optoelectron.*, **9**, 432 (2014).
20. V.A.Skryshevsky, Yu.S.Milovanov, I.V.Gavrilchenko et al., *Phys. Status Solidi A*, **212**, 1941 (2015).